Check for updates

Received: 5 October 2021 | Revised: 31 January 2022 | Accepted: 5 February 2022

DOI: 10.1111/nan.12800

ORIGINAL ARTICLE

Neuropathology and Applied Neurobiology
JOURNAL OF THE BRITISH NEUROPATHOLOGICAL SOCIETY

WILEY

# Intrathecal amyloid-beta oligomer administration increases tau phosphorylation in the medial temporal lobe in the African green monkey: A nonhuman primate model of Alzheimer's disease

Dustin R. Wakeman[1] | Michael R. Weed[1] | Sylvia E. Perez[2] | Erika N. Cline[3] | Kirsten L. Viola[3] | Kyle C. Wilcox[3] | David S. Moddrelle[4] | Ernell Z. Nisbett[4] | Anish M. Kurian[1] | Amanda F. Bell[4] | Ricaldo Pike[4] | Peer B. Jacobson[5] | William L. Klein[3] | Elliott J. Mufson[2] | Matthew S. Lawrence[1] | John D. Elsworth[1]

[1]Virscio Inc., New Haven, Connecticut, USA

[2]Neurobiology, Barrow Neurological Institute, Phoenix, Arizona, USA

[3]Neurobiology, Northwestern University, Evanston, Illinois, USA

[4]Virscio Inc., St. Kitts Biomedical Research Foundation, St. Kitts, West Indies

[5]AbbVie, North Chicago, Illinois, USA

**Correspondence**
John Elsworth, Virscio Inc., Science Park, New Haven, CT, USA.
Email: jelsworth@virscio.com

**Funding information**
NIH, Grant/Award Numbers: R43 OD023025, R44 AG067832, P01 AG014449

## Abstract

**Aims:** An obstacle to developing new treatment strategies for Alzheimer's disease (AD) has been the inadequate translation of findings in current AD transgenic rodent models to the prediction of clinical outcomes. By contrast, nonhuman primates (NHPs) share a close neurobiology with humans in virtually all aspects relevant to developing a translational AD model. The present investigation used African green monkeys (AGMs) to refine an inducible NHP model of AD based on the administration of amyloid-beta oligomers (AβOs), a key upstream initiator of AD pathology.

**Methods:** AβOs or vehicle were repeatedly delivered over 4 weeks to age-matched young adult AGMs by intracerebroventricular (ICV) or intrathecal (IT) injections. Induction of AD-like pathology was assessed in subregions of the medial temporal lobe (MTL) by quantitative immunohistochemistry (IHC) using the AT8 antibody to detect hyperphosphorylated tau. Hippocampal volume was measured by magnetic resonance imaging (MRI) scans prior to, and after, intrathecal injections.

**Results:** IT administration of AβOs in young adult AGMs revealed an elevation of tau phosphorylation in the MTL cortical memory circuit compared with controls. The largest increases were detected in the entorhinal cortex that persisted for at least 12 weeks after dosing. MRI scans showed a reduction in hippocampal volume following AβO injections.

**Conclusions:** Repeated IT delivery of AβOs in young adult AGMs led to an accelerated AD-like neuropathology in MTL, similar to human AD, supporting the value of this translational model to de-risk the clinical trial of diagnostic and therapeutic strategies.

KEYWORDS
African green monkey, Alzheimer's disease, amyloid-beta oligomer, entorhinal cortex, hippocampus, intrathecal, phosphorylated Tau

 © 2022 British Neuropathological Society 

## INTRODUCTION

Alzheimer's disease (AD) currently affects 50 million people worldwide with a projected increase to over 150 million by 2050. Yet despite the immense socioeconomic burden (US $1 trillion in 2018 alone), there are no available treatments that address the progression of this devastating disease [1,2]. In fact, only five drugs have made it to the US and European markets in the last 15 years, none of which have had any effect on slowing or halting disease progression and its debilitating cognitive decline. This lack of therapeutic treatments remains despite a tremendous influx of research funding from both government institutions and biopharmaceutical companies. Disappointingly, the past few years have seen a series of failures of Phase 2 and Phase 3 clinical trials [3,4]. Most experts have argued that the failure to achieve clinical efficacy relates to the choice of drug target, disease stage and critically lack of clinically predictive animal models that accurately mimic both disease pathology and concomitant neurocognitive decline with associated analytic endpoints [5–8].

Amyloid beta (Aβ) plaques, aggregates of the Aβ peptide, were originally thought to be the toxic entity in AD and consequently, it was discouraging when clinical trials targeting the build-up of Aβ plaques did not halt cognitive decline in treated patients [9,10]. These disappointing outcomes have refocused efforts to understand other mechanisms leading to AD neurodegeneration and its related cognitive impairment. A recent consensus is that amyloid plaques and tau neurofibrillary tangles are likely non-toxic protein cellular aggregates and that their soluble oligomer precursors, amyloid β oligomers (AβOs) and oligomeric tau are the toxic agents that result in synaptic and neuronal degeneration [11–14]. The biological activity of tau, which includes the stabilisation of microtubules and the coordinated movement of molecules along the microtubule, is tightly regulated by phosphorylation. In AD, tau is abnormally hyperphosphorylated, which promotes tau self-association and the eventual formation of tau oligomers, leading to pathology [15,16]. Interestingly, evidence indicating that AβOs promote tau phosphorylation [13,17–20] suggests the importance of testing whether AβOs play a role in the initiation of tau pathogenesis in a nonhuman primate (NHP) model of AD.

Currently, mouse models dominate preclinical AD research and have contributed to important advances in the field. However, the majority of these models are based on genetic forms of AD and do not recapitulate the full spectrum and clinical course of the disease, especially the complex cognitive impairments seen in patients with sporadic AD [7,21–23]. This caveat likely contributed to the lack of efficacy in clinical amyloid vaccination trials [9,21,22,24–26]. Therefore, there is an urgent need to develop an NHP model of AD to guide the development of effective treatments for this disease [27]. Advantages of a NHP model include greater homology to human genomics, immune response, neuronal network complexity, cognitive processing, synaptic regulation, pharmacokinetics and pharmacodynamics [28–32]. Furthermore, there are distinct differences between rodents and NHPs in terms of the biochemistry, physiology, anatomy of key brain regions affected by AD [28,29,32–35]. It is also relevant that changes occurring in the NHP brain during ageing resemble certain aspects of AD pathology [36–38]. While some NHPs develop cortical Aβ plaques later in life during natural ageing [39–41], the accumulation of pathological tauopathy is rare [38,42–46]. The finding of amyloid deposits in the aged NHP brain suggests a permissive internal milieu that supports the development of AD-like lesions. However, inconsistencies in the occurrence of AD lesions, timescale and expense of accruing a large population of aged NHPs render a naturally occurring NHP model of AD impractical for most preclinical drug development programmes. To overcome these caveats [40,47], there is a need to develop a model of AD that can be induced in normal, young adult NHPs.

Early attempts to study AD pathogenesis in NHPs relied upon the intracerebroventricular (ICV) injection of fibrillar Aβ in aged [39,48] or the intracerebral delivery of a brain homogenate derived from an AD patient into adult NHPs [49]. However, neither model displayed tau pathology. Recently, tau and other signs of AD-like pathology were described in the neo- and limbic cortex in cynomolgus (*Macaca fascicularis*) and rhesus (*Macaca mulatta*) monkeys 1 week after receiving repeated ICV delivery of AβOs [50–52], which are small, diffusible aggregates of the Aβ peptide that accumulate in the AD brain [53,54]. Although a promising proof-of-concept, it remains unknown whether this approach can initiate

### Key Points

- An obstacle to developing new treatment strategies for Alzheimer's disease (AD) has been the inadequate translation of findings in current AD transgenic rodent models to the prediction of clinical outcomes.
- The present investigation used African green monkeys (AGMs) to refine an inducible nonhuman primate model of AD based on the administration of amyloid-beta oligomers (AβOs), a key upstream initiator of AD pathology.
- Lumbar intrathecal (IT) administration of AβOs in young adult AGMs revealed an elevation of tau phosphorylation in the medial temporal lobe cortical memory circuit compared with controls, which persisted for at least 12 weeks after dosing.
- MRI scans showed a reduction in hippocampal volume following AβO injections compared with controls.
- These data indicate that repeated IT delivery of AβOs in young adult AGMs led to an accelerated AD-like neuropathology in MTL, similar to human AD, supporting the value of this translational model to de-risk the clinical trial of diagnostic and therapeutic strategies.

longer term AD-like tau changes that are amenable to large-scale preclinical pharmacological studies to prevent or reverse AβO-induced pathogenesis. Therefore, we sought to develop a more reproducible and robust AβO test system using the African green monkey (AGM) that is suitable for long-term drug discovery including cognitive and tissue-based neuropathology assessments [55].

To accomplish this, we performed a study that consisted of five objectives: (1) confirm that ICV administration of ABOs induces pTau expression in AGMs; (2) determine whether intrathecal (IT) delivery of AβOs to the central nervous system (CNS) of AGMs is a viable experimental strategy to model aspects of AD pathology; (3) determine whether IT administration of AβOs to awake or sedated AGMs [56] produce different AD-like phenotypes; (4) determine the effect of frequency of AβO delivery on AD-like neuropathology in AGMs; and (5) determine the persistence of AβO induced AD-like changes following the cessation of dosing. The main outcome measures are induction of phosphorylated tau (pTau) determined by quantitative immunohistochemistry (IHC) and change in hippocampal volume measured by magnetic resonance imaging (MRI).

## MATERIALS AND METHODS

### Subjects

Adult male AGMs or vervets (*Chlorocebus aethiops sabaeus*) were either colony-born or sourced from the free-ranging population located on the island of St. Kitts, West Indies. Age estimation was based on a set of physical criteria that has been calibrated using AGMs of known ages that were born at the colony (see Supporting information). Male AGMs were randomised by age (mean and SEM; AβO group $9.9 \pm 0.6$ years, controls $9.8 \pm 0.6$ years) and weight (mean and SEM: AβO group $5.6 \pm 0.2$ kg, controls $5.8 \pm 0.2$ kg). None of the monkeys used here were in the age range in which we and others [37,38,45,46,57] have typically seen pathological alterations associated with ageing. The surgery necessary for ICV and IT administrations is described in Supporting information.

### AβO production and validation

AβO's were prepared and validated by Northwestern University, Chicago, IL (WLK). The initial characterisation of AβOs prepared by this method (see Supporting information) included assessment of size distribution of AβOs by western blot and atomic force microscopy (Figure 1), confirmation of AβO identity, solubility and size distribution following freezing by top-down mass spectrometry, western blot and size exclusion high pressure liquid chromatography (Figures S1 and S2), and the ability of AβO preparations following freeze-thawing to induce tau phosphorylation, alter spine morphology in cell cultures and disrupt hippocampal-related memory function when injected ICV into mice (Figures S3 and S4). Although subsequent batches of AβOs were not screened by all of these techniques, each preparation used in this study was evaluated for size distribution, stability and solubility upon freeze-thawing and potency in the cell culture assay. Multiple vials of AβOs, each containing the target dose for a single injection (100 or 200 μg, depending on the study objective), and vehicle (2% v/v dimethyl sulphoxide in phosphate-buffered saline) were shipped in a liquid nitrogen vapour shipper to the St. Kitts Biomedical Research Foundation and stored below −70°C. AβOs and vehicle were thawed in a 37°C bead-bath for 5 min followed by centrifugation for 10 min at 14,000 rcf at 4°C. Prior to dosing, vials were stored on wet ice until solutions were withdrawn into a syringe and delivered to the animal. All injections were made within 2 h of thawing the AβOs or vehicle solutions.

### ICV administration of AβOs

Monkeys were randomly stratified into two groups: ICV surgery with either AβO treatment ($n = 2$) or vehicle treatment ($n = 2$). Details of the surgical methods are provided in Supporting information. After a 2–3 week ICV post-surgery recovery period, AβO or vehicle was injected subcutaneously through the septum of the access port. The target dose was 100-μg AβO per injection, and the actual dose delivered was calculated from the volume retrieved from each injection vial. The actual mean AβO dose delivered at 50 μl/min was 99 μg (in 260 μl of vehicle) or the same volume of vehicle alone as well as a 500-μl sterile saline flush, three times a week for 4 weeks.

### IT lumbar spinal cord AβO administration

Over time, the monkeys to be dosed while awake were gradually adapted to placement in a primate restraint chair (Primate Products, Miami, FL, USA) [60]. Details of the surgery necessary for IT dosing are provided in Supporting information. Two to three weeks after surgery, sedated or awake monkeys received IT dosing of AβO or vehicle through the septum of the access port either once or three times a week for a total of 4 weeks followed by 1-ml sterile saline flush. Monkeys receiving AβO or vehicle were balanced by age and weight (see Supporting information). After dosing, chair-trained monkeys were maintained in the prone position for 20 min to promote drug delivery to the brain via the cerebrospinal fluid (CSF) [61], before being returned to their home cages. The target dose of AβO was 200 μg per injection. The actual dose was calculated from the volume retrieved from each injection vial. Two cohorts of monkeys were dosed by the IT route. The first cohort received an average of 186-μg AβO in 491 μl of vehicle (or vehicle alone) and the second received an average of 172-μg AβO in 740-μl vehicle (or vehicle alone) (Table 1). To

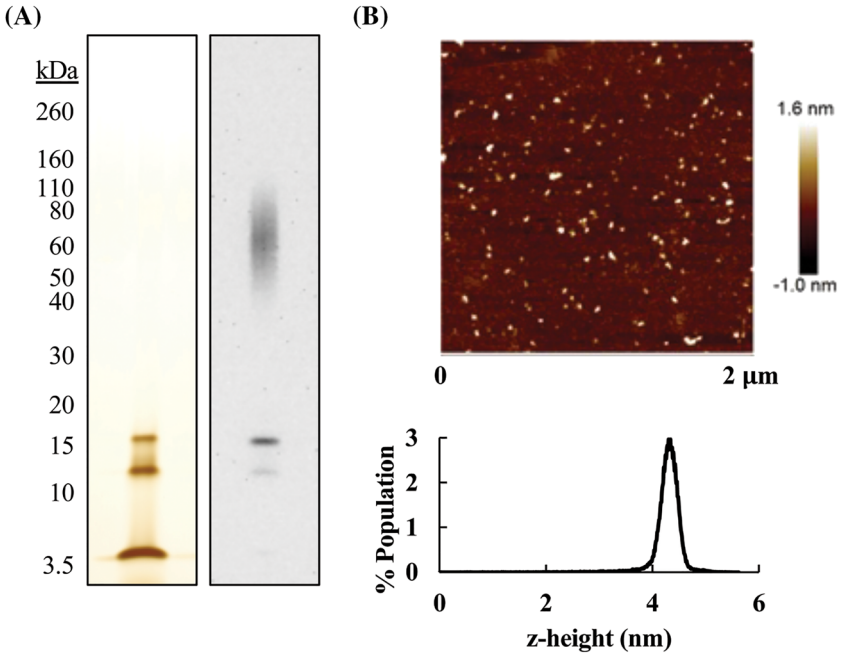


**FIGURE 1** Assessment of size distribution of AβO preparation. (A) AβOs resolved on a 4–20% Tris-glycine polyacrylamide gel at 15 (Western, right panel) or 45 ([silver stain, left panel] pmol/well). Immunoreactivity to an AβO-specific antibody (NU2) [58] is shown. (B) Atomic force microscopy (AFM) shows that under non-denaturing conditions, the AβO preparation is globular and uniform in s-height, 4.33 ± 0.13 nm, which is comparable to previous reports [59]

**TABLE 1** AGM dosing cohorts

| Group size | Dosing article | Injection frequency (number/week for 4 weeks) | Status (during dosing) | Termination (after last dose) |
|---|---|---|---|---|
| ICV cohort | | | | |
| 2 | AβO | 3× | Sedated | 1 week |
| 2 | Vehicle | 3× | Sedated | 1 week |
| Uninjected ICV cohort | | | | |
| 5 | N/A | N/A | N/A | N/A |
| IT Cohort 1 | | | | |
| 3 | AβO | 3× | Sedated | 1 week |
| 1 | AβO | 3× | Sedated | 4 weeks |
| 2 | AβO | 3× | Awake | 1 week |
| 5 | AβO | 1× | Sedated | 1 week |
| 2 | AβO | 1× | Awake | 1 week |
| 2 | Vehicle | 3× | Sedated | 1 week |
| 2 | Vehicle | 1× | Sedated | 1 week |
| IT Cohort 2 | | | | |
| 2 | AβO | 3× | Awake | 1 week |
| 5 | AβO | 3× | Awake | 4 weeks |
| 3 | AβO | 3× | Awake | 12 weeks |
| 1 | Vehicle | 3× | Awake | 1 week |
| 1 | Vehicle | 3× | Awake | 4 weeks |
| 1 | Vehicle | 3× | Awake | 12 weeks |
| Uninjected IT cohort | | | | |
| 2 | N/A | N/A | N/A | N/A |

confirm that surgery and injections did not elevate baseline pTau, the first cohort also included two monkeys matched for age and sex that did not undergo surgery. Optical density (OD) of pTau immunoreactivity in medial temporal lobe (MTL) regions in these monkeys fell within the range measured in vehicle-treated monkeys. These two monkeys were included in the control group for subsequent analyses of AβO-induced changes in pTau immunoreactivity.

### Immunohistochemistry

Details of the methods used for brain collection and IHC are provided in Supporting information. Briefly, brain slabs containing the MTL were sectioned on a freezing sliding microtome in the coronal plane at 40 microns into six adjacent series and stored in cryoprotectant. Sections were immunostained using AT8, CP13 and Alz-50 [62] for the evaluation of tau [63], 6E10, which recognises both APP/Aβ, MOAB-2 [64] and $A\beta_{1-42}$ to examine Aβ pathology, as well as glia markers Iba1 and GFAP to evaluate inflammatory response (see Supporting information).

### OD measurements

Sections from half series per case were immunostained in parallel for pTau immunoreactivity using AT8. For IT Cohort 1, the spread and intensity of staining in the MTL was rated blinded to treatment. A semi-quantitative binary rating system divided monkeys into two groups; one that displayed dark and another light and less widely spread tau immunoreactivity. Effect of dosing on pTau AT8 immunoreactivity in MTL subregions (i.e., outer or superficial layers [I–III] of the entorhinal cortex [ENT-O], inner or deeper entorhinal cortical layers [V-VI] [ENT-I], CA1, CA2/3 subfields of hippocampus, and subicular [Sub] neurons [C] and fibres [F] areas) was quantitatively evaluated while blinded to treatment using optical densitometry in both cohorts. Sections used for this analysis were processed in parallel to avoid batch-to-batch differences in chemicals and IHC procedural variables. OD measurements of tau profiles were performed in one field covering an area of 0.40 $mm^2$ at 40× magnification in the fields of interest (ENT-O, ENT-I, CA1, CA2/3, Sub-C and Sub-F) displaying strong AT8 immunostaining in an average of 14 sections per case as previously described [42,65]. Background measurements from the corpus callosum were averaged and subtracted from the mean OD values for each immunostained section. All quantitation and photography were performed with the aid of a Nikon Eclipse microscope coupled with NIS-Elements Imaging software (Nikon, Japan).

### MRI scans

Accuracy of ICV and IT placement was confirmed by the visualisation of an MRI signal produced by injection of a gadolinium-based contrast agent though the ICV or IT access ports prior to dosing with AβO or vehicle. Briefly, 0.3 ml of Magnevist (Bayer Healthcare Pharmaceuticals) diluted 1:100 with sterile saline was injected followed by a saline flush (0.5 ml for ICV ports, 1 ml for IT ports) and MRI scans were performed using a Philips Intera 1.5 Tesla machine. Monkeys in both IT cohorts had 3D TFE (turbo field echo) MRI scans without contrast before dosing and again during the week prior to study termination. The mean volume of left and right hippocampus in each animal was measured by an MRI data analyst (AMK) blinded to treatment, using manual segmentation commercial tomography software (Amira software, ThermoFisher).

### Statistical analysis

Parametric statistical tests (*t* test, one- and two-way ANOVA) were used for comparisons of continuous dependent variables (i.e., for OD values of AT8 immunoreactivity in tissue from Cohort 1 plus Cohort 2 and for hippocampal volumes determined by MRI). Non-parametric tests (Chi-squared) were used for comparison of categorical data (AT8 immunoreactivity data from cohort 1 only). The particular test used for each specific comparison is stated in the appropriate section in Results. For all analyses, the result was considered statistically significant only if the *p* value was less than the alpha level of 0.05.

## RESULTS

### pTau changes following ICV administration of AβOs in AGMs

ICV injection of AβOs resulted in an increase in pTau AT8 immunoreactivity in the MTL in AGMs compared with controls (Figure 2), consistent with ICV AβO administration in the cynomolgus monkey [52]. Because ICV delivery of AβO in the AGM induced an accelerated expression of AT8, an early marker of tau phosphorylation associated with pretangles [63,66], these data provide support for the use of this NHP species to study the onset of induced tau.

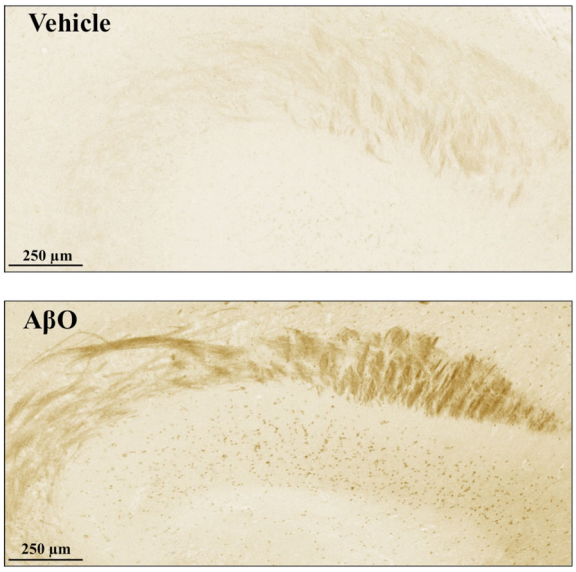


**FIGURE 2** AT8 immunostained fascicles (brown) coursing within the in hippocampus of an African green monkey (AGM) that received either intracerebroventricular (ICV) AβOs or vehicle injections. Note the greater AT8 immunoreactivity in the AβO compared with the vehicle-treated AGM

## IT administration of AβOs in AGMs

### Qualitative observations of tau profiles

To avoid the invasive surgical procedure necessary to delivery repeated ICV injections, we investigated the less complex and more reliable IT dosing route for administration of AβOs. Here we found granular/punctate AT8 cytoplasmic immunoreactivity in the perikarya, processes and fibres in the hippocampus, molecular layer of the dentate gyrus, entorhinal cortex and subiculum, with less immunoreactivity in the CA1 field of the hippocampus in AβO-injected monkeys, and to a lesser degree in vehicle-injected AGMs (Figure 3). Overall hippocampal AT8 immunostaining was greater following IT AβO treatment three times a week in sedated and awake compared with control AGMs (Figure 3A–C). A band of AT8-ir fibres was observed within hippocampal CA2/CA3 subfield in both sedated (Figure 3B) and non-sedated animals. Cytoplasmic AT8 immunostaining was seen in subicular neurons in sedated (Figure 3D,E) and awake animals (Figure 3F). Cellular processes and fibres were also seen in the subiculum (Figure 3A,B,D–F) and entorhinal cortex Layers I to V in AβO-injected sedated and awake monkeys (Figure 3G,H), while staining in the vehicle-injected animals appeared mainly in Layers I and II of the entorhinal cortex (Figure 3I,J). In addition, a few AT8-positive neurons were detected in the entorhinal cortex in awake (Figure 3H inset) and

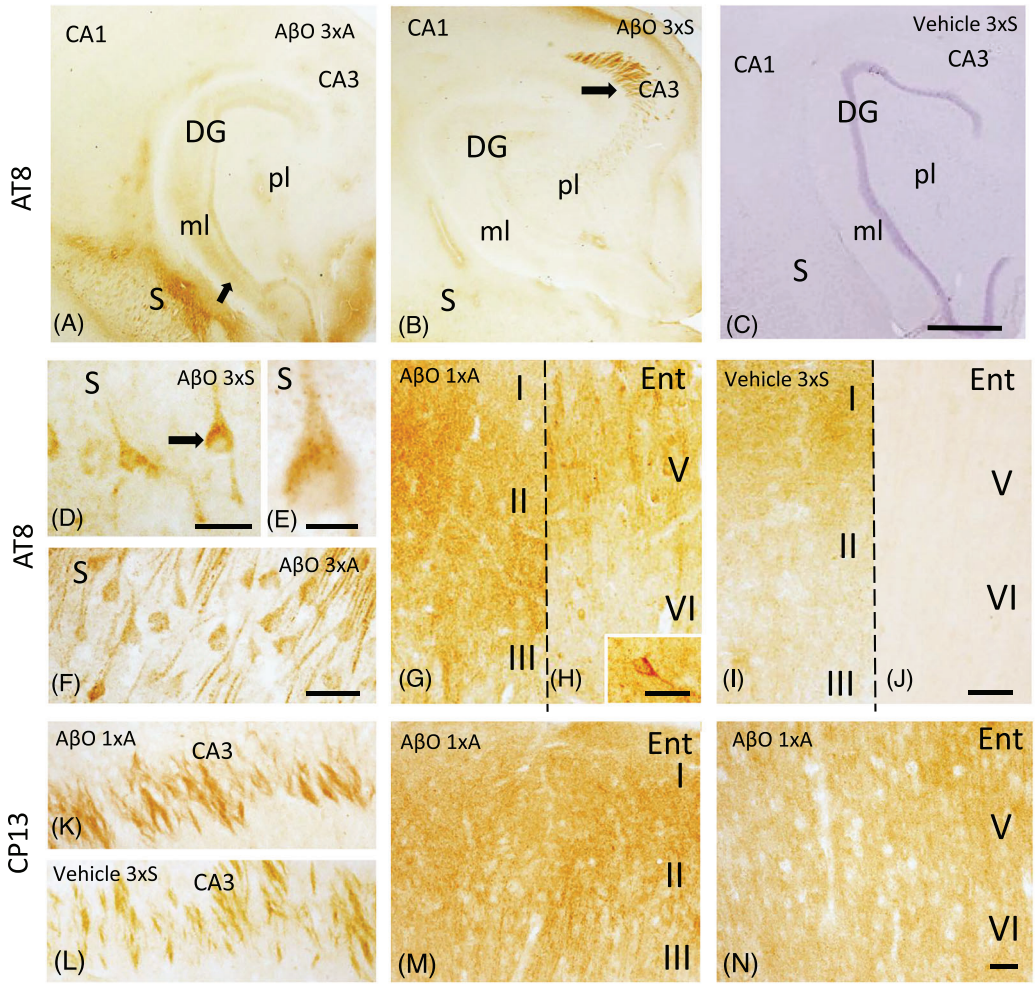


**FIGURE 3** Panels (A–C) Hippocampal images showing greater AT8 immunoreactivity in the subiculum (S) and molecular layer of the dentate gyrus (arrow) in an awake (A) compared with a sedated (B) AβO-injected African green monkey (AGM). Note the lack of AT8 immunoreactivity in a Gill's haematoxylin counterstained section from a vehicle-injected AGM (C). Note the intense band of AT8 staining (arrow) seen in the CA3 subfield of the hippocampus in a sedated AβO-injected AGM (B). (D–F): Subicular neurons displaying AT8 cytoplasmic reactivity in a sedated (D, E) and an awake (F) AβO-injected AGM. (E) Higher magnification image of the AT8-positive subicular neuron seen in Panel (D) (arrow). (G–J) Entorhinal cortex showing stronger AT8 immunoreactivity in Layers I, II, V and VI in an awake AβO-injected (G,H) compared with a sedated vehicle-injected AGM (I,J). Inset in Panel (H) shows an AT8 entorhinal cortex positive neuron in an awake AβO-injected AGM. (K,I) Images showing a dense band of CP13 immunoreactivity within the hippocampal CA3 subfield in an awake AβO-treated (K) compared with lesser immunoreactivity in a vehicle-treated (I) AGM. (M,N) CP13 immunoreactivity in entorhinal cortex Layers I to VI in an awake AβO-treated AGM. Abbreviations: 3 × A, three times per week awake; 3 × S, three times per week sedated; 1 × A, once per week awake; CA1, CA3 subfields of the hippocampus; DG, dentate gyrus; Ent, entorhinal cortex; pl, polymorphic layer of the DG; ml, molecular layer of the DG; S, subiculum. Scale bars: C = 1000 μm and applies to A and B, D and F = 25 μm, E = 10 μm, J = 50 μm and applies to G–I, inset = 20 μm, *n* = 50 μm and applies to K–M

sedated AβO-injected AGMs. Granular CP13 pTau immunostaining was observed in the perikarya, processes and fibres in a similar pattern to that seen for AT8 in the MTL of AGMs. CP13 immunoreactivity was also observed in fibre bundles in the hippocampal CA2/CA3 subfield (Figure 3K,L), entorhinal cortex (Figure 3M,N) and subiculum, but less immunoreactivity was detected in CA1 similar to AT8. By contrast, Alz-50 immunoreactivity was not found in these regions, consistent with the temporal relationship between early phosphorylational compared with later conformational (Alz-50, data not shown) events that occur during the evolution of tau pathology in NHP and humans [67,68].

## Quantification of IT AβO pTau induction in different cohorts of AGMs

Because qualitative pTau observations showed an increase in AT8 immunostaining in AβO-treated AGMs compared with controls, the effects were quantitatively examined using a binary rating system and OD measurements in two AGM cohorts. Cohorts of either awake or sedated AGMs received IT injections of AβOs or vehicle at two different dosing intervals (once a week or three times a week for 4 weeks) and were terminated at different time points (1, 4 or 12 weeks) after the last dose (Table 1).

***Cohort 1***: IT delivery of AβOs resulted in an increase in pTau immunoreactivity in AD-relevant MTL regions in the AGM compared with controls (Figure 2). Chi-squared analysis of the data derived from the binary rating system (see Materials and Methods) found significantly greater AT8 pTau immunostaining in monkeys that received AβOs while awake compared with controls (Chi-squared analysis $\chi^2$ [df2, $N = 18$] $= 7.0$, $p = 0.03$; Figure S5). In addition, there was a trend for more frequent administration of AβO to be associated with more intense MTL AT8 immunostaining, although this relationship did not reach statistical significance (Figure S5).

***Cohorts 1 and 2***: To quantify the effect of AβO dosing variables on AT8 immunostaining, sections from both cohorts were immunoreacted in parallel followed by OD measurements in the ENT-O ENT-I, CA1, CA2/3 hippocampal subfield tract and subiculum. Two-way ANOVA of OD values from each of six MTL regions per monkey ($n = 23$ AβO-treated, $n = 9$ controls) revealed a significant increase in AT8 immunoreactivity in AβO-treated compared with controls monkeys [$F(1,180) = 7.6$, $p < 0.01$] and a significant effect of brain region [$F(5,180) = 39.6$, $p < 0.001$], but no treatment by region interaction [$F(5,180) = 1.1$]. Because OD values for AT8 immunoreactivity from a single control and an AβO-treated monkey were noticeably higher than others in their treatment groups for each region, we used the Grubbs test, which detects outliers in a univariate data set assumed to come from a normally distributed population; these monkeys were deviant from their respective groups and were excluded from subsequent analyses. After removal of these cases from the analysis, treatment [$F(1,168) = 16.1$, $p < 0.0001$] and region [$F(5,168) = 40.7$, $p < 0.0001$] effects remained significant and a treatment by region interaction became significant [$F(5,168) = 3.2$, $p = 0.01$]. The significant main effects of treatment, region and their interaction confirm that AβO administration resulted in an increase in AT8 immunoreactivity (Figure 4). Post-hoc comparison with Šidák's test indicated a significant difference between AβO-treated and control animals in the ENT-O region, with trends towards significance in other regions. The percentage increase in AT8 OD compared with controls for each region ranged between 25% and 67%, with the greatest increase in tau immunoreactivity occurring in the ENT-O (Figure 5). Summing ODs for all six regions per monkey revealed a mean overall increase in AT8 reactivity of 37% in AβO-treated compared with control monkeys.

## Timing and state of consciousness upon tau after final AβO injection

We also examined whether AT8 immunoreactivity was influenced by the length of time after the last AβO injection (three time points), the number of AβO injections (two regimens) or state of consciousness (awake or sedated). Due to the limitation in the number of monkeys in the 12 possible experimental combinations (e.g., no awake or sedated monkeys were terminated at 4 or 12 weeks after a single weekly dosing paradigm) (Table 1), we were only able to the compare the effect of time after AβO injection in a subset of animals at each of the three time points on AT8 immunoreactivity. This included monkeys injected three times a week for 4 weeks with AβOs while awake and terminated either at 1 ($n = 3$), 4 ($n = 5$) or 12 ($n = 3$) weeks after final injection. One-way ANOVA revealed that the sum of AT8 OD measurements in the six MTL regions examined was not significantly different between the three time points [$F(2,8) = 0.22$], indicating that AT8 protein levels remain

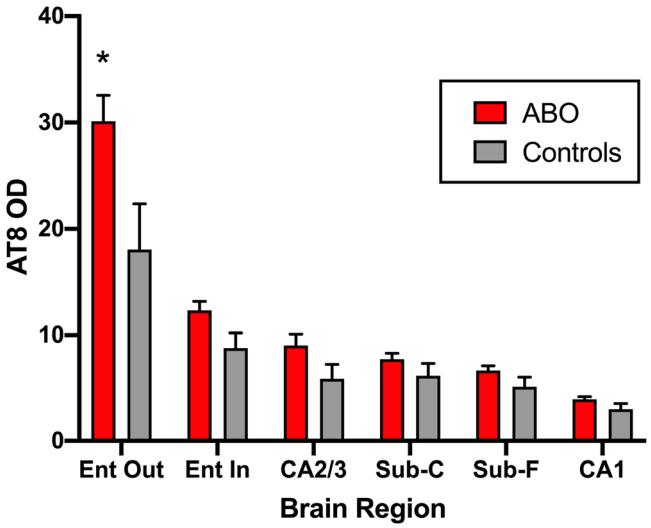


**FIGURE 4** Optical density measurement of AT8 immunoreactivity following AβO IT administration ($n = 22$) compared with control African green monkeys (AGMs) ($n = 8$) within the medial temporal lobe (MTL) in Cohorts 1 and 2. Mean value ± SE is shown. * denotes significant effect of AβO compared with controls

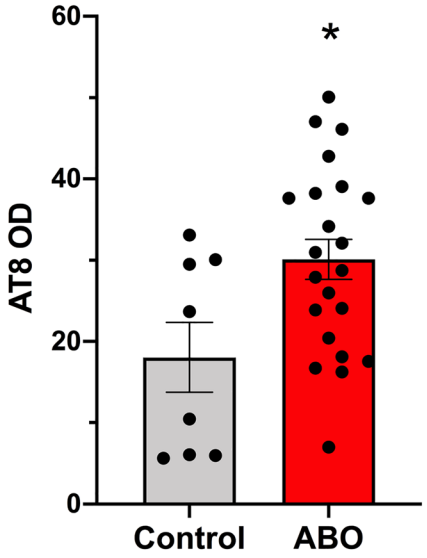


**FIGURE 5** Optical density measurement showing greater intensity of AT8 immunoreactivity in the outer layers of the entorhinal cortex in monkeys administered IT AβOs ($n = 22$) compared with controls ($n = 8$); mean ± SE and individual values shown, * denotes significantly greater than controls

stable between 1 and 12 weeks after AβO administration. A sub-analysis with the dependent variable restricted to OD values only from the ENT-O (the region displaying the most pronounced AβO-induced pTau) revealed a significantly greater AT8 signal at 4 and 12 weeks compared with 1 week [$F(2,8) = 4.5$, $p < 0.05$]. In order to examine the effect of the other dosing variables (frequency of injections and awake/sedated status) on AT8 staining, data were collapsed across study termination time-points to increase statistical power. These analyses (unpaired two-tailed $t$ test) revealed that neither frequency of injection [$t(20) = 0.87$] nor awake/sedated status [$t(20) = 0.74$] had a significant effect on AT8 immunoreactivity across the region of the MTL.

## Qualitative analysis of amyloid and glial pathology following IT AβO injection in AGMs

APP/Aβ (6E10) immunoreactivity revealed diffuse-like plaques in the MTL (e.g., hippocampus and entorhinal cortex), amygdala (Figure S6) and neocortex. By contrast, staining using the MOAB-2 antibody, which is specific for Residues 1–4 of Aβ and does not cross react with APP [64], as well as the antibody against the C-terminal of $A\beta_{1-42}$ resulted in negative immunostaining (Figure S6), suggesting that these deposits consist mainly of APP or APP derivatives, and to a lesser extent Aβ species. In addition, microglia and astrocytes were immunostained using antibodies against Iba1 and GFAP, respectively. Light microscopic evaluation revealed greater Iba1 and GFAP immunostaining only in the dentate gyrus polymorphic layer in both IT AβO-injected sedated and awake compared with vehicle-injected AGMs (Figure S7).

## Repeat IT AβO administration reduces hippocampal volume in AGMs

MRI scans were analysed to determine the effect of AβO or vehicle treatment on hippocampal volume in AGMs. ANOVA of the data derived from MRI scans revealed a significant effect of interval between baseline and terminus [$F = 19.6(1,23)$, $p < 0.0005$] among treatment groups on hippocampal volume. Further Šidák's multiple comparison test revealed a reduction in hippocampal volume for the group terminated 4 weeks after AβO injections [$t(23) = 3.3$, $p < 0.05$] (Figure 6).

## Safety and tolerability of repeat IT administration of AβOs in AGMs

All AGMs remained healthy throughout the duration of the study. AβO administration was well tolerated with no adverse effects or change in general health or wellness behaviours. There was no significant difference in body weight (6.0 ± 0.6 kg) at the time of surgery between the ICV and IT animals [one-way ANOVA $F(2,36) = 2.7$]. Statistical analysis of time between surgery and monkeys terminated 1 week after final ICV or IT dose revealed a significant difference in body weight between procedures [unpaired two-tailed $t$ test, $t(24) = 5.0$, $p < 0.0001$], with IT surgery maintaining weight more consistently than those undergoing ICV surgery (Figure 7).

# DISCUSSION

The current results provide several advances in modelling AD pathology in NHPs, which are urgently needed to avoid the continued failure

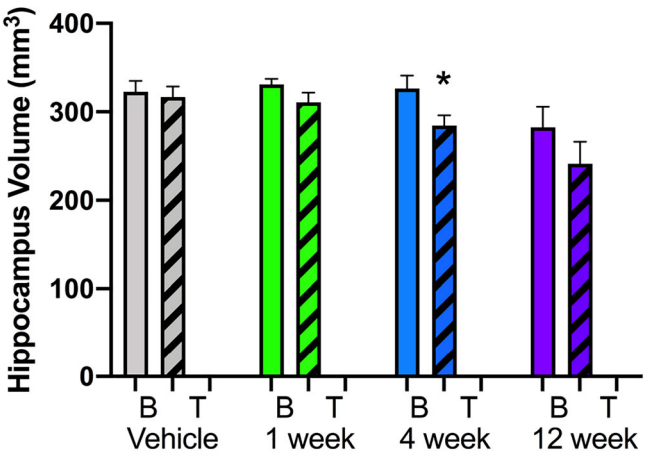


**FIGURE 6** Magnetic resonance imaging (MRI)-based hippocampal volume before injections (B) and at termination (T) in African green monkeys (AGMs) receiving an intrathecal (IT) vehicle ($n = 6$) or AβO injection at 1 week ($n = 13$), 4 weeks ($n = 5$) or 12 weeks ($n = 3$) after the last injection. * denotes significant decrease between B and T at the 4-week time point

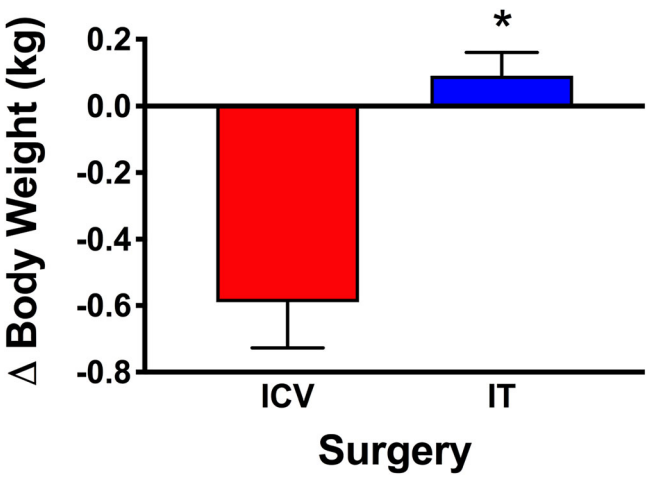


**FIGURE 7** Mean change in body weight (±*SD*) between surgery to implant subcutaneous access ports and 1 week after the last intracerebroventricular (ICV) ($n = 9$) or intrathecal (IT) ($n = 14$) dosing; this represents all animals for which these paired measurements were taken. In addition to there being a group difference in change of body weight, the ICV group significantly lost weight between surgery and 1 week after the last dose. * denotes significant difference between groups

of treatments advanced to the clinic based largely on data derived from transgenic mouse models of AD. The present report confirms that repeated ICV administration of AβOs to male AGMs induces increased pTau (AT8) immunoreactivity in the MTL compared with controls similar to that reported for female cynomolgus monkeys [52], implying that species and sex of an Old World monkey are not critical determinants underlying the development of an NHP AβO model of AD. Based on our findings that ICV AβO injection induced an increase in pTau protein reactivity in the MTL of the AGM, we investigated whether IT delivery of AβOs, a less invasive delivery route with reduced risk of CNS injury related to ICV surgical access, would evoke a similar pTau/AT8 immunoprofile in the AGM brain. Here, we provide novel findings showing that IT delivery of AβOs in two different relatively large cohorts of monkeys produced a significant elevation of AT8 immunoreactivity in the MTL compared with age-matched controls. Interestingly, the AT8 immunoreactivity was most pronounced in the entorhinal cortex. Furthermore, we obtained evidence that the pTau elevations persist for at least 12 weeks following the last AβO dose. Neither the frequency (1 vs. 3 times a week for 4 weeks) nor state of consciousness (awake vs. sedated) during AβO dosing significantly affected the degree of pTau reactivity. MRI analysis revealed a significant loss of hippocampal volume during the course of the study suggesting a further macroscopic effect of AβOs upon brain structure. Overall, the present findings establish IT AβO delivery to the AGM as a model for the investigation of tau pathology and strategies to prevent the onset and/or progression of AD.

Previous studies have used various species of aged macaque or AGMs, which over their life span display Aβ plaques [38,40,69–71] but to a lesser degree tau pathology [37,57,72] to model AD pathogenesis. Studies in Old World monkeys indicate that Aβ plaques are not typically observed until after middle age (≥ about 15 years) and rarely in animals as young as those used in the current investigation (mean age 10 years) (see Supporting information). In the present study, there was a lack of Aβ (MOAB-2 antibody) and $Aβ_{1-42}$ positive plaques, while diffuse 6E10 immunoreactive accumulations were observed in the MTL of AβO and vehicle IT-treated young adult AGMs supporting previous studies [71]. However, we found granular/punctate AT8 cytoplasmic immunoreactivity in perikarya and processes in the hippocampus, entorhinal cortex and subiculum in AβO, but to a lesser degree in vehicle treated monkeys. In fact, we found a significant increase in AT8 immunoreactivity in the entorhinal cortex and subiculum in AβO-injected AGMs. In addition, granular pTau CP13 immunostaining, but not the later conformational tau isoform Alz-50, was seen in the entorhinal cortex, subiculum and hippocampus in both treated and non-treated young adult monkeys. Thioflavin S, a stain of β-pleated sheet conformation characteristic of NFTs and senile plaques, failed to reveal positive profiles in the MTL in any of the AGMs examined (data not shown) [42]. Together, these findings suggest that AβOs induce a pretangle form of tau in the MTL in the AGM monkey. Interestingly, a recent study revealed limited granular AT8-tau immunoreactivity in small round cells mainly in the lateral temporal cortex and, to a lesser extent, within the subsectors of the entorhinal cortex in middle-age (mean 11.2 years) and old (mean 21.7 years) AGMs [38]. The different phenotype of AT8 labelled neurons between this and the present study suggest differences in method of fixation and tissue processing. In fact, the authors of the earlier study [38] suggested that formalin fixation may have affected tau immunostaining resulting in non-specific labelling. In the current investigation, tissue was immersion fixed in buffered 4% paraformaldehyde solution and processed as free floating sections compared with paraffin-embedded tissue [38]. In fact, the manner by which a brain is fixed (transcardial or immersion), type of fixative, and cutting process (paraffin vs frozen) affects tau immunostaining [73]. Interestingly, we found an absence of AT8 immunoreactivity in paraffin-embedded tissue in the MTL in middle-age and older AGMs (unpublished observations). Studies using electron microscopy have reported limited tau-bearing positive tangles in the entorhinal cortex in the aged rhesus macaque monkey [57], while tau immunoreactive neurons have been reported in cortex of aged great apes (i.e., gorillas and chimpanzees) [42,74]. Here, we demonstrate that the MTL of AGMs display only limited pTau immunoreactivity, but that AβO administration produced greater reactivity to this protein in the entorhinal cortex and subiculum making these NHPs a potential model to evaluate treatments that would slow or prevent the evolution of tau pathologies. Moreover, we observed diffuse deposits of APP/Aβ and glial markers in MTL, but further studies are ongoing to quantify the longitudinal relationship between these markers following AβO injection in the AGM.

Another approach to modelling AD is the ICV injection of fibrillar Aβ into the NHP brain but this method failed to reproduce classic AD lesions [39,48]. However, several studies in rhesus or cynomolgus monkeys demonstrated that ICV injection of AβOs produced several of the cardinal features of AD including synapse loss, astrocytic and

microglia activation and intracellular accumulation of tau in neo and limbic cortex [50–52,75]. Notably, ICV AβO injection in the rhesus monkey induced synaptotoxicity and microglia activation in dorsolateral prefrontal cortex and dentate gyrus of the hippocampus, but not tau pathology in either of these areas [51], suggesting that tau-based pathology is not an inevitable consequence of AβO injection. However, these studies did not report on the animals' cognitive status, which prevents the ability to determine an association between neuropathologic lesions and cognition. Overall, these findings suggest that the application of AβO ICV injections in NHPs induces many of the pathological features seen in human AD making this species a potential model to study neuropathobiology, cognitive impairment and treatment approaches for AD.

As discussed above, intracranial or ICV injections of AβOs or other inducing agents [49,76] in the NHP brain demonstrate the usefulness of these delivery methods in developing a primate correlate of AD [50–52]. Such procedures require accurate sterile stereotaxic surgery, ideally guided by MRI scans, as monkey brains exhibit significant inter-animal anatomical variability. In addition to the challenge of securing and stabilising a catheter in the lateral ventricles that results in a reliable CSF flow, the ICV approach has an inherent risk associated with inserting a cannula through the depth of the brain parenchyma [77] and associated induction of brain changes through physical disruption. Although the less invasive spinal IT delivery method offers a solution to the drawbacks of the ICV procedure, injecting AβOs intrathecally has the potential to dilute AβOs before reaching relevant CNS targets. The flow of CSF from the lumbar spinal cord to the brain is well established [78], and IT administration of certain drugs, including recombinant proteins, are widely distributed within the brain parenchyma to achieve pharmacologically relevant levels [61,79,80]. Factors that affect CSF flow include changes in blood volume in intracranial arteries [81–83], inspiration [84–88], venous pulsatility and total cerebral blood flow, some of which are enhanced in the horizontal compared with an upright position [56,89]. Because animals that are awake during an IT injection exhibit greater respiration rate, heart rate, blood pressure, body movement and CSF production [90] compared with sedated monkeys, we investigated whether NHPs receiving IT injection of AβOs while awake and maintained in a horizontal position displayed enhanced brain pTau. Preliminary data from Cohort 1 suggested that awake-dosing with AβOs led to greater AT8 immunostaining compared with those that were sedated. However, we did not discern a difference between awake or sedated IT-injected animals when data were combined from Cohorts 1 and 2, indicating that state of consciousness does not significantly affect the ability of AβOs to induce pTau expression in the MLT when delivered by the IT route. Similarly, the frequency of AβO dosing during the 4-week treatment period did not have a significant effect upon the degree of pTau in the MTL, demonstrating that a single weekly IT injection (∼200-μg AβO) was sufficient to up-regulate pTau.

The onset of abnormal tau within the brain following AβO administration is an important parameter that dictates study design and type of AD therapeutics to be tested in a NHP model. In order to gauge the persistence of elevated pTau induced by AβOs, we terminated our experimental groups at different weekly intervals (1, 4, or 12 weeks) following the final dose. We found that the effect of AβOs on tau induction persists for at least 12 weeks following the last dose. Because prior studies have not extended beyond 1 week after final dose [50–52], the current findings provide the first evidence of protracted elevations in pTau and glial pathology in an NHP AβO model of AD.

In AD, there is a characteristic pattern of tau lesion progression, which can be identified by spread of increased numbers of AT8-positive neurofibrillary tangles initiated in the transentorhinal cortex and then within the entorhinal-hippocampal complex [63]. In the current model, we found greater AT8 reactivity in the outer layers of entorhinal cortex, with similar trends in other MTL regions, which is consistent with that seen in AD [63]. Although the absence of definitive Aβ plaques or frank neurofibrillary tangles suggests that AβOs induce early phases of tau pathogenesis, further research is needed to confirm this in our NHP model of AD. In this regard, having an AGM AβO model to test therapeutics targeting early cellular tau phosphorylation events during the onset of AD would be extremely beneficial.

The exact mechanism responsible for the spread of tau lesions in the MTL in AD is not fully understood. Because AβOs are elevated in the AD brain [91], it is possible that these proteins act as templates to seed or cross-seed oligomer formation derived from peptide monomers. The hypothesis of neuron-to-neuron transfer of oligomers and propagation by seeding offers an explanation for the predictable pattern of tau lesions across the MTL connectome in AD [92–94]. However, whether the exogenous delivery of AβOs to the brain via uptake from the CSF underlies aggregate self-propagation in the NHP brain remain to be determined. Because presumably there are similarities between human and AGM AβOs, studies with labelled exogenous AβOs are needed to address oligomer propagation in the NHP brain.

MRI images offer a potential valuable *in vivo* biomarker to determine the effect of AβOs upon brain structure in the current AβO NHP model. MRI brain scans were taken before injections and just prior to study termination. Analysis of these scans revealed a significant decrease in hippocampal volume that persisted at least 4 weeks after AβO delivery. While the magnitude of this change was relatively small, it is notable that the same percentage loss was observed over a 6–12-month period in people with mild cognitive impairment compared with aged controls [95]. A recent MRI study identified an age-related reduction in the volume of several brain regions that was associated with Aβ and phospho-tau burden in AGMs [38]. Future studies are needed to explore the cellular components that underlie the volumetric MRI changes seen in AβO-treated monkeys compared with controls. Ongoing and future studies will pursue a more detailed MRI analysis and other potentially valuable in-life biomarkers (e.g., CSF and plasma analytes) and automated detection of cognitive deficits using touchscreen-testing devices in the AGM AβO model of AD-like tau pathology.

The current findings suggest that IT administration of standardised AβOs induces elevated pTau in the MTL memory circuit that persisted for up to 12 weeks following the final oligomer treatment in young adult AGMs. Moreover, frequency of injections over 4 weeks or state of consciousness during treatment did not affect outcome measures. In addition, repeated MRI scans revealed a reduction in hippocampal volume following AβO injections. The innovative IT NHP model of AβO delivery induces tau immunoreactivity reminiscent of that seen during the early stage of human AD in the MTL providing a valuable translational resource to test novel diagnostic and therapeutic strategies in a manner that will significantly de-risk clinical trials.

## ACKNOWLEDGEMENTS

This study was jointly supported by Virscio Inc., AbbVie and NIH SBIR grants to Virscio Inc. (R43OD023025, R44AG067832) and PO1 AG014449 (EJM). The authors acknowledge the excellent assistance provided by Benjie A. Culp, Tatiana M. Corey, Darnel J. Allen, Phill J. Cooper, Eleanor M. Demmons, Xavier G. Morton, Garim K.T. Jones, and Vincia M. Woods at the St. Kitts Biomedical Research Foundation, by Jennifer Miguel at the Barrow Neurological Institute and by Luis F. Schachner, Nadia DiNunno and Maíra Assunção at Northwestern University. Antech Diagnostics (Southaven, MS) and Ross University School of Veterinary Medicine (St Kitts, West Indies) were valuable resources for haematology and clinical chemistry assays.

## CONFLICT OF INTEREST

The authors declare that they have no competing interests with the content of the manuscript.

## AUTHOR CONTRIBUTIONS

D.R.W., M.R.W., K.C.W., P.B.J., J.D.E.: design of the study, data analysis, data interpretation. W.L.K., M.S.L.: design of the study, data interpretation. D.S.M., E.S.N., R.P.: surgical method development and implementation, animal evaluation and selection. A.F.B., A.M.K.: MRI method development, implementation and data analysis. S.E.P., E.J.M.: sample analysis, data analysis, and data interpretation. E.N.C., K.L.V.: sample analysis, data analysis. Principal authors of manuscript: D.R.W., M.R.W., E.N.C., S.E.P., E.J.M., M.S.L., J.D.E. All authors approved and/or provided edits to the manuscript

## ETHICS STATEMENT

All studies described were approved by the appropriate Institutional Animal Care and Use Committee, ensuring that research was conducted in accordance with the highest scientific, humane and ethical principles.

## DATA AVAILABILITY STATEMENT

The data that support the findings of this study are available from the corresponding author upon reasonable request.

## ORCID

*John D. Elsworth* https://orcid.org/0000-0002-0323-0886

## REFERENCES

1. Alzheimer's Association. 2019 Alzheimer's disease facts and figures: https://www.alz.org/media/documents/alzheimers-facts-and-figures-2019-r.pdf
2. Patterson C. The state of the art of dementia research: new frontiers. *Alzheimer's Disease International*. 2018;4-46.
3. Cummings JL, Morstorf T, Zhong K. Alzheimer's disease drug-development pipeline: few candidates, frequent failures. *Alzheimers Res Ther*. 2014;6(4):37. doi:10.1186/alzrt269
4. Panza F, Lozupone M, Logroscino G, Imbimbo BP. A critical appraisal of amyloid-beta-targeting therapies for Alzheimer disease. *Nat Rev Neurol*. 2019;15(2):73-88. doi:10.1038/s41582-018-0116-6
5. Zhang L, Chen C, Mak MS, et al. Advance of sporadic Alzheimer's disease animal models. *Med Res Rev*. 2019;40(1):431-458. doi:10.1002/med.21624
6. Yiannopoulou KG, Anastasiou AI, Zachariou V, Pelidou SH. Reasons for failed trials of disease-modifying treatments for Alzheimer disease and their contribution in recent research. *Biomedicine*. 2019;7(4):97. doi:10.3390/biomedicines7040097
7. Mullane K, Williams M. Preclinical models of Alzheimer's disease: relevance and translational validity. *Curr Protoc Pharmacol*. 2019;84(1):e57. doi:10.1002/cpph.57
8. Cummings J. Lessons learned from Alzheimer disease: clinical trials with negative outcomes. *Clin Transl Sci*. 2018;11(2):147-152. doi:10.1111/cts.12491
9. Salloway S, Sperling R, Fox NC, et al. Bapineuzumab, clinical trial I. Two phase 3 trials of bapineuzumab in mild-to-moderate Alzheimer's disease. *N Engl J Med*. 2014;370(4):322-333. doi:10.1056/NEJMoa1304839
10. Vandenberghe R, Rinne JO, Boada M, et al. Bapineuzumab, clinical study I. Bapineuzumab for mild to moderate Alzheimer's disease in two global, randomized, phase 3 trials. *Alzheimers Res Ther*. 2016;8(1):18. doi:10.1186/s13195-016-0189-7
11. Querfurth HW, LaFerla FM. Alzheimer's disease. *N Engl J Med*. 2010;362(4):329-344. doi:10.1056/NEJMra0909142
12. Chiti F, Dobson CM. Protein misfolding, amyloid formation, and human disease: a summary of progress over the last decade. *Annu Rev Biochem*. 2017;86(1):27-68. doi:10.1146/annurev-biochem-061516-045115
13. Cline EN, Bicca MA, Viola KL, Klein WL. The amyloid-beta oligomer hypothesis: beginning of the third decade. *J Alzheimers Dis*. 2018;64(s1):S567-S610. doi:10.3233/JAD-179941
14. Lambert MP, Barlow AK, Chromy BA, et al. Diffusible, nonfibrillar ligands derived from Aβ1–42 are potent central nervous system neurotoxins. *Proc Natl Acad Sci U S A*. 1998;95(11):6448-6453. doi:10.1073/pnas.95.11.6448
15. Miao J, Shi R, Li L, et al. Pathological tau from Alzheimer's brain induces site-specific hyperphosphorylation and SDS- and reducing agent-resistant aggregation of tau in vivo. *Front Aging Neurosci*. 2019;11:34. doi:10.3389/fnagi.2019.00034
16. Guerrero-Munoz MJ, Gerson J, Castillo-Carranza DL. Tau oligomers: the toxic player at synapses in Alzheimer's disease. *Front Cell Neurosci*. 2015;9:464. doi:10.3389/fncel.2015.00464
17. Bloom GS. Amyloid-beta and tau: the trigger and bullet in Alzheimer disease pathogenesis. *JAMA Neurol*. 2014;71(4):505-508. doi:10.1001/jamaneurol.2013.5847
18. De Felice FG, Wu D, Lambert MP, et al. Alzheimer's disease-type neuronal tau hyperphosphorylation induced by Aβ oligomers. *Neurobiol Aging*. 2008;29(9):1334-1347. doi:10.1016/j.neurobiolaging.2007.02.029
19. Kametani F, Hasegawa M. Reconsideration of amyloid hypothesis and tau hypothesis in Alzheimer's disease. *Front Neurosci*. 2018;12:25. doi:10.3389/fnins.2018.00025
20. Pickett EK, Herrmann AG, McQueen J, et al. Amyloid beta and tau cooperate to cause reversible behavioral and transcriptional deficits

in a model of Alzheimer's disease. *Cell Rep* 2019;29:3592-604 e5. doi:10.1016/j.celrep.2019.11.044
21. Hall AM, Roberson ED. Mouse models of Alzheimer's disease. *Brain Res Bull*. 2012;88(1):3-12. doi:10.1016/j.brainresbull.2011.11.017
22. Mangialasche F, Solomon A, Winblad B, Mecocci P, Kivipelto M. Alzheimer's disease: clinical trials and drug development. *Lancet Neurol*. 2010;9(7):702-716. doi:10.1016/S1474-4422(10)70119-8
23. Dawson TM, Golde TE, Lagier-Tourenne C. Animal models of neurodegenerative diseases. *Nat Neurosci*. 2018;21(10):1370-1379. doi:10.1038/s41593-018-0236-8
24. LaFerla FM, Oddo S. Alzheimer's disease: Aβ, tau and synaptic dysfunction. *Trends Mol Med*. 2005;11(4):170-176. doi:10.1016/j.molmed.2005.02.009
25. Selkoe DJ. Resolving controversies on the path to Alzheimer's therapeutics. *Nat Med*. 2011;17(9):1060-1065. doi:10.1038/nm.2460
26. Zahs KR, Ashe KH. Too much good news'—are Alzheimer mouse models trying to tell us how to prevent, not cure, Alzheimer's disease? *Trends Neurosci*. 2010;33(8):381-389. doi:10.1016/j.tins.2010.05.004
27. King A. The search for better animal models of Alzheimer's disease. *Nature*. 2018;559(7715):S13-S15. doi:10.1038/d41586-018-05722-9
28. Ergorul C, Levin LA. Solving the lost in translation problem: improving the effectiveness of translational research. *Curr Opin Pharmacol*. 2013;13(1):108-114. doi:10.1016/j.coph.2012.08.005
29. Geerts H. Of mice and men: bridging the translational disconnect in CNS drug discovery. *CNS Drugs*. 2009;23(11):915-926. doi:10.2165/11310890-000000000-00000
30. Izpisua Belmonte JC, Callaway EM, Caddick SJ, et al. Brains, genes, and primates. *Neuron*. 2015;86(3):617-631. doi:10.1016/j.neuron.2015.03.021
31. Phillips KA, Bales KL, Capitanio JP, et al. Why primate models matter. *Am J Primatol*. 2014;76(9):801-827. doi:10.1002/ajp.22281
32. Wendler A, Wehling M. The translatability of animal models for clinical development: biomarkers and disease models. *Curr Opin Pharmacol*. 2010;10(5):601-606. doi:10.1016/j.coph.2010.05.009
33. Passingham R, Wise S. *The Prefrontal Cortex: Anatomy, Evolution, and the Origin of Insight*: Oxford University Press. 2012. doi:10.1093/acprof:osobl/9780199552917.001.0001
34. Rosene D, Van Hoesen G. The hippocampal formation of the primate brain. some comparative aspects of architecture and connections. In *The Cerebral Cortex* Eds. E Jones, A Peters. New York: Plenum Press. 1987:345–456. doi:10.1007/978-1-4615-6616-8_9
35. Wakeman DR, Crain AM, Snyder EY. Large animal models are critical for rationally advancing regenerative therapies. *Regen Med*. 2006;1(4):405-413. doi:10.2217/17460751.1.4.405
36. Chen JA, Fears SC, Jasinska AJ, et al. Neurodegenerative disease biomarkers Aβ1–40, Aβ1–42, tau, and p-tau181 in the vervet monkey cerebrospinal fluid: relation to normal aging, genetic influences, and cerebral amyloid angiopathy. *Brain Behav*. 2018;8(2):e00903 doi:10.1002/brb3.903
37. Cramer PE, Gentzel RC, Tanis KQ, et al. Aging African green monkeys manifest transcriptional, pathological, and cognitive hallmarks of human Alzheimer's disease. *Neurobiol Aging*. 2018;64:92-106. doi:10.1016/j.neurobiolaging.2017.12.011
38. Latimer CS, Shively CA, Keene CD, et al. A nonhuman primate model of early Alzheimer's disease pathologic change: implications for disease pathogenesis. *Alzheimers Dement*. 2019;15(1):93-105. doi:10.1016/j.jalz.2018.06.3057
39. Geula C, Wu CK, Saroff D, Lorenzo A, Yuan M, Yankner BA. Aging renders the brain vulnerable to amyloid β-protein neurotoxicity. *Nat Med*. 1998;4(7):827-831. doi:10.1038/nm0798-827
40. Lemere CA, Beierschmitt A, Iglesias M, et al. Alzheimer's disease abeta vaccine reduces central nervous system Aβ levels in a non-human primate, the Caribbean vervet. *Am J Pathol*. 2004;165(1):283-297. doi:10.1016/S0002-9440(10)63296-8
41. Podlisny MB, Tolan DR, Selkoe DJ. Homology of the amyloid beta protein precursor in monkey and human supports a primate model for beta amyloidosis in Alzheimer's disease. *Am J Pathol*. 1991;138(6):1423-1435.
42. Perez SE, Raghanti MA, Hof PR, et al. Alzheimer's disease pathology in the neocortex and hippocampus of the western lowland gorilla (*Gorilla gorilla gorilla*). *J Comp Neurol*. 2013;521(18):4318-4338. doi:10.1002/cne.23428
43. Edler MK, Sherwood CC, Meindl RS, et al. Aged chimpanzees exhibit pathologic hallmarks of Alzheimer's disease. *Neurobiol Aging*. 2017;59:107-120. doi:10.1016/j.neurobiolaging.2017.07.006
44. Heuer E, Rosen RF, Cintron A, Walker LC. Nonhuman primate models of Alzheimer-like cerebral proteopathy. *Curr Pharm Des*. 2012;18(8):1159-1169. doi:10.2174/138161212799315885
45. Oikawa N, Kimura N, Yanagisawa K. Alzheimer-type tau pathology in advanced aged nonhuman primate brains harboring substantial amyloid deposition. *Brain Res*. 2010;1315:137-149. doi:10.1016/j.brainres.2009.12.005
46. Uchihara T, Endo K, Kondo H, et al. Tau pathology in aged cynomolgus monkeys is progressive supranuclear palsy/corticobasal degeneration- but not Alzheimer disease-like-ultrastructural mapping of tau by EDX. *Acta Neuropathol Commun*. 2016;4(1):118. doi:10.1186/s40478-016-0385-5
47. Frost JL, Le KX, Cynis H, et al. Pyroglutamate-3 amyloid-beta deposition in the brains of humans, non-human primates, canines, and Alzheimer disease-like transgenic mouse models. *Am J Pathol*. 2013;183(2):369-381. doi:10.1016/j.ajpath.2013.05.005
48. Leung E, Guo L, Bu J, Maloof M, El Khoury J, Geula C. Microglia activation mediates fibrillar amyloid-beta toxicity in the aged primate cortex. *Neurobiol Aging*. 2011;32(3):387-397. doi:10.1016/j.neurobiolaging.2009.02.025
49. Baker HF, Ridley RM, Duchen LW, Crow TJ, Bruton CJ. Induction of beta (A4)-amyloid in primates by injection of Alzheimer's disease brain homogenate. Comparison with transmission of spongiform encephalopathy. *Mol Neurobiol*. 1994;8(1):25-39. doi:10.1007/BF02778005
50. Batista AF, Forny-Germano L, Clarke JR, et al. The diabetes drug liraglutide reverses cognitive impairment in mice and attenuates insulin receptor and synaptic pathology in a non-human primate model of Alzheimer's disease. *J Pathol*. 2018;245(1):85-100. doi:10.1002/path.5056
51. Beckman D, Ott S, Donis-Cox K, et al. Oligomeric Aβ in the monkey brain impacts synaptic integrity and induces accelerated cortical aging. *Proc Natl Acad Sci U S A*. 2019;116(52):26239-26246. doi:10.1073/pnas.1902301116
52. Forny-Germano L, Lyra e Silva NM, Batista AF, et al. Alzheimer's disease-like pathology induced by amyloid-β oligomers in nonhuman primates. *J Neurosci*. 2014;34(41):13629-13643. doi:10.1523/JNEUROSCI.1353-14.2014
53. Gong Y, Chang L, Viola KL, et al. Alzheimer's disease-affected brain: presence of oligomeric Aβ ligands (ADDLs) suggests a molecular basis for reversible memory loss. *Proc Natl Acad Sci U S A*. 2003;100(18):10417-10422. doi:10.1073/pnas.1834302100
54. Selkoe DJ, Hardy J. The amyloid hypothesis of Alzheimer's disease at 25 years. *EMBO Mol Med*. 2016;8(6):595-608. doi:10.15252/emmm.201606210
55. Jasinska AJ, Schmitt CA, Service SK, et al. Systems biology of the vervet monkey. *ILAR J*. 2013;54(2):122-143. doi:10.1093/ilar/ilt049
56. Barten D, Cadelina G, Weed M. Dosing, collection and quality control issues in cerebrospinal fluid research using animal models. In: Deisenhammer F, Teunissen C, Tumani H, eds. *Cerebrospinal Fluid in Neurological Disorders*. Elsevier. 2017:47–66. doi:10.1016/B978-0-12-804279-3.00004-6

57. Paspalas CD, Carlyle BC, Leslie S, et al. The aged rhesus macaque manifests Braak stage III/IV Alzheimer's-like pathology. *Alzheimers Dement*. 2018;14(5):680-691. doi:10.1016/j.jalz.2017.11.005
58. Lambert MP, Velasco PT, Chang L, et al. Monoclonal antibodies that target pathological assemblies of Aβ. *J Neurochem*. 2007;100(1): 23-35. doi:10.1111/j.1471-4159.2006.04157.x
59. Chromy BA, Nowak RJ, Lambert MP, et al. Self-assembly of Aβ(1–42) into globular neurotoxins. *Biochemistry*. 2003;42(44):12749-12760. doi:10.1021/bi030029q
60. McMillan JL, Bloomsmith MA, Prescott MJ. An international survey of approaches to chair restraint of nonhuman primates. *Comp Med*. 2017;67(5):442-451.
61. Barten DM, Cadelina GW, Weed MR. Dosing, collection, and quality control issues in cerebrospinal fluid research using animal models. *Handb Clin Neurol*. 2017;146:47-64. doi: 10.1016/B978-0-12-804279-3.00004-6
62. Jicha GA, Bowser R, Kazam IG, Davies P. Alz-50 and MC-1, a new monoclonal antibody raised to paired helical filaments, recognize conformational epitopes on recombinant tau. *J Neurosci Res*. 1997; 48(2):128-132. doi:10.1002/(SICI)1097-4547(19970415)48:2<128::AID-JNR5>3.0.CO;2-E
63. Braak H, Braak E. Staging of Alzheimer's disease-related neurofibrillary changes. *Neurobiol Aging*. 1995;16(3):271-278; discussion 8-84. doi:10.1016/0197-4580(95)00021-6
64. Youmans KL, Tai LM, Kanekiyo T, et al. Intraneuronal Aβ detection in 5xFAD mice by a new Aβ-specific antibody. *Mol Neurodegener*. 2012; 7(1):8. doi:10.1186/1750-1326-7-8
65. Miguel JC, Perez SE, Malek-Ahmadi M, Mufson EJ. Cerebellar calcium-binding protein and neurotrophin receptor defects in down syndrome and alzheimer's disease. *Front Aging Neurosci*. 2021;13. doi:10.3389/fnagi.2021.645334
66. Koss DJ, Dubini M, Buchanan H, Hull C, Platt B. Distinctive temporal profiles of detergent-soluble and -insoluble tau and Aβ species in human Alzheimer's disease. *Brain Res*. 2018;1699:121-134. doi: 10.1016/j.brainres.2018.08.014
67. Carmel G, Mager EM, Binder LI, Kuret J. The structural basis of monoclonal antibody Alz50's selectivity for Alzheimer's disease pathology. *J Biol Chem*. 1996;271(51):32789-32795. doi: 10.1074/jbc.271.51.32789
68. Mondragon-Rodriguez S, Basurto-Islas G, Santa-Maria I, et al. Cleavage and conformational changes of tau protein follow phosphorylation during Alzheimer's disease. *Int J Exp Pathol*. 2008;89(2):81-90. doi:10.1111/j.1365-2613.2007.00568.x
69. Kumar S, Frost JL, Cotman CW, et al. Deposition of phosphorylated amyloid-beta in brains of aged nonhuman primates and canines. *Brain Pathol*. 2018;28(3):427-430. doi:10.1111/bpa.12573
70. Merrill DA, Masliah E, Roberts JA, et al. Association of early experience with neurodegeneration in aged primates. *Neurobiol Aging*. 2011;32(1):151-156. doi:10.1016/j.neurobiolaging.2009.01.014
71. Kalinin S, Willard SL, Shively CA, et al. Development of amyloid burden in African Green monkeys. *Neurobiol Aging*. 2013;34(10):2361-2369. doi:10.1016/j.neurobiolaging.2013.03.023
72. Darusman HS, Gjedde A, Sajuthi D, et al. Amyloid β1–42 and the phoshorylated tau threonine 231 in brains of aged cynomolgus monkeys (*Macaca fascicularis*). *Front Aging Neurosci*. 2014;6:313. doi: 10.3389/fnagi.2014.00313
73. Oh KJ, Perez SE, Lagalwar S, Vana L, Binder L, Mufson EJ. Staging of Alzheimer's pathology in triple transgenic mice: a light and electron microscopic analysis *Int J Alzheimers Dis* 2010;2010, 1-24. doi: 10.4061/2010/780102
74. Perez SE, Miguel JC, He B, et al. Frontal cortex and striatal cellular and molecular pathobiology in individuals with Down syndrome with and without dementia. *Acta Neuropathol*. 2019;137(3):413-436. doi: 10.1007/s00401-019-01965-6
75. Lourenco MV, Clarke JR, Frozza RL, et al. TNF-alpha mediates PKR-dependent memory impairment and brain IRS-1 inhibition induced by Alzheimer's beta-amyloid oligomers in mice and monkeys. *Cell Metab*. 2013;18(6):831-843. doi:10.1016/j.cmet.2013.11.002
76. Beckman D, Chakrabarty P, Ott S, et al. A novel tau-based rhesus monkey model of Alzheimer's pathogenesis. *Alzheimers Dement*. 2021;17(6):933-945. doi:10.1002/alz.12318
77. Slavc I, Cohen-Pfeffer JL, Gururangan S, et al. Best practices for the use of intracerebroventricular drug delivery devices. *Mol Genet Metab*. 2018;124(3):184-188. doi:10.1016/j.ymgme.2018.05.003
78. Dichiro G. Movement of the cerebrospinal fluid in human beings. *Nature*. 1964;204(4955):290-291. doi:10.1038/204290a0
79. Haga PT, Pizzichelli G, Mortensen M, et al. A numerical investigation of intrathecal isobaric drug dispersion within the cervical subarachnoid space. *PLoS ONE*. 2017;12(3):e0173680. doi:10.1371/journal.pone.0173680
80. Calias P, Banks WA, Begley D, Scarpa M, Dickson P. Intrathecal delivery of protein therapeutics to the brain: a critical reassessment. *Pharmacol Ther*. 2014;144(2):114-122. doi:10.1016/j.pharmthera.2014.05.009
81. Brinker T, Stopa E, Morrison J, Klinge P. A new look at cerebrospinal fluid circulation. *Fluids Barriers CNS*. 2014;11(1):10. doi: 10.1186/2045-8118-11-10
82. Strik C, Klose U, Erb M, Strik H, Grodd W. Intracranial oscillations of cerebrospinal fluid and blood flows: analysis with magnetic resonance imaging. *J Magn Reson Imaging*. 2002;15(3):251-258. doi: 10.1002/jmri.10084
83. Klarica M, Rados M, Erceg G, Petosic A, Jurjevic I, Oreskovic D. The influence of body position on cerebrospinal fluid pressure gradient and movement in cats with normal and impaired craniospinal communication. *PLoS ONE*. 2014;9(4):e95229. doi:10.1371/journal.pone.0095229
84. Daouk J, Bouzerar R, Baledent O. Heart rate and respiration influence on macroscopic blood and CSF flows. *Acta Radiol*. 2017;58(8): 977-982. doi:10.1177/0284185116676655
85. Dreha-Kulaczewski S, Joseph AA, Merboldt KD, Ludwig HC, Gartner J, Frahm J. Inspiration is the major regulator of human CSF flow. *J Neurosci*. 2015;35(6):2485-2491. doi: 10.1523/JNEUROSCI.3246-14.2015
86. Dreha-Kulaczewski S, Konopka M, Joseph AA, et al. Respiration and the watershed of spinal CSF flow in humans. *Sci Rep*. 2018;8(1): 5594. doi:10.1038/s41598-018-23908-z
87. Simon MJ, Iliff JJ. Regulation of cerebrospinal fluid (CSF) flow in neurodegenerative, neurovascular and neuroinflammatory disease. *Biochim Biophys Acta*. 2016;1862(3):442-451. doi:10.1016/j.bbadis.2015.10.014
88. Takizawa K, Matsumae M, Sunohara S, Yatsushiro S, Kuroda K. Characterization of cardiac- and respiratory-driven cerebrospinal fluid motion based on asynchronous phase-contrast magnetic resonance imaging in volunteers. *Fluids Barriers CNS*. 2017;14(1):25. doi: 10.1186/s12987-017-0074-1
89. Papisov MI, Belov VV, Gannon KS. Physiology of the intrathecal bolus: the leptomeningeal route for macromolecule and particle delivery to CNS. *Mol Pharm*. 2013;10(5):1522-1532. doi: 10.1021/mp300474m
90. Liu G, Mestre H, Sweeney AM, et al. Direct measurement of cerebrospinal fluid production in mice. *Cell Rep*. 2020;33(12):108524. doi: 10.1016/j.celrep.2020.108524
91. Tomic JL, Pensalfini A, Head E, Glabe CG. Soluble fibrillar oligomer levels are elevated in Alzheimer's disease brain and correlate with cognitive dysfunction. *Neurobiol Dis*. 2009;35(3):352-358. doi: 10.1016/j.nbd.2009.05.024

92. Friesen M, Meyer-Luehmann M. Aβ seeding as a tool to study cerebral amyloidosis and associated pathology. *Front Mol Neurosci*. 2019;12:233. doi:10.3389/fnmol.2019.00233
93. Hashimoto M, Ho G, Takamatsu Y, et al. Possible role of amyloid cross-seeding in evolvability and neurodegenerative disease. *J Parkinsons Dis*. 2019;9(4):793-802. doi:10.3233/JPD-191675
94. Jucker M, Walker LC. Self-propagation of pathogenic protein aggregates in neurodegenerative diseases. *Nature*. 2013;501(7465):45-51. doi:10.1038/nature12481
95. Schuff N, Woerner N, Boreta L, et al. Alzheimer's disease neuroimaging I. MRI of hippocampal volume loss in early Alzheimer's disease in relation to ApoE genotype and biomarkers. *Brain*. 2009;132(4):1067-1077. doi:10.1093/brain/awp007

## SUPPORTING INFORMATION

Additional supporting information may be found in the online version of the article at the publisher's website.

**How to cite this article:** Wakeman DR, Weed MR, Perez SE, et al. Intrathecal amyloid-beta oligomer administration increases tau phosphorylation in the medial temporal lobe in the African green monkey: A nonhuman primate model of Alzheimer's disease. *Neuropathol Appl Neurobiol*. 2022;e12800. doi:10.1111/nan.12800